Assessment of exposure to airborne carbon nanotubes by laser-induced breakdown spectroscopy analysis of filter samples

Jean-Baptiste Sirven, P. Dewalle, C. Quere, V. Fauvet, M. Tabarant, S. Motellier, L. Golanski, A. Guiot, M. Amdaoud, Simon Clavaguera, et al.

Journal Name

ARTICLE

Assessment of exposure to airborne carbon nanotubes by laser-induced breakdown spectroscopy analysis of filter samples

J.-B. Sirven[a], P. Dewalle[a], C. Quéré[a], V. Fauvet[b], M. Tabarant[a]

S. Motellier[c], L. Golanski[c], A. Guiot[c], M. Amdaoud[c], S. Clavaguera[c]

A. Roynette[d], S. Pontreau[d], F.-X. Ouf[d], and F. Gensdarmes[d].

Exposure assessment is a key step in the evaluation of the risk induced by the handling of engineered nanomaterials. It is a very complex task, because several properties of nanoparticles are assumed to have an effect on their hazard. For exposure monitoring at workplace, real-time onsite measurements are commonly implemented to measure the particles size and number density, whereas the sampled material is subsequently analysed by electron microscopy. A complementary approach would consist in doing onsite chemical analysis of the filter samples, in order to routinely monitor a potential chronic exposure. Laser-induced breakdown spectroscopy (LIBS) has distinctive advantages for that purpose. Therefore, this work aims at evaluating the performances of LIBS to assess the exposure to airborne carbon nanotubes (CNTs) at workplace. As carbon is a ubiquitous element in the environment, our strategy was to target metal impurities of CNTs, aluminum and iron in our case. Then, we proceeded in three steps. First, we optimized the choice of the filter type to get the lowest detection limit for both elements. Secondly, this filter was used to quantitatively measure deposited CNTs. Eventually, we conducted an onsite measurement campaign in an industrial CNTs production plant to evaluate the exposure in a real situation. We demonstrated that we could reach a detection limit for CNTs compliant with the current NIOSH recommendation of 1 µg/m^3, and that the detected CNTs during the onsite campaign in areas accessible to workers were at an extremely low concentration, several orders of magnitude lower than this recommendation.

JB_Sirven_2017-1.tif

After graduate studies in optics, Jean-Baptiste Sirven discovered the world of elemental analysis during his PhD at University Bordeaux 1 on the detection of heavy metals in soils by laser-induced breakdown spectroscopy (LIBS). When he defended it in 2006, he did not suspect that more than 10 years later he would still be working on this fascinating technique, so simple and so complex at the same time. One member of his thesis jury introduced him at the French Alternative Energies and Atomic Energy Commission (CEA) as a post-doc researcher, where he became a member of the ChemCam team and briefly contributed to the development of the Martian LIBS instrument. When CEA decided to keep him as a permanent fellow, he switched to more down-to-earth, but equally challenging research topics of interest in the nuclear field, where LIBS is a relevant option for a number of applications. His current favorite subjects cover fundamentals of laser ablation and LIBS, development of multivariate methods for LIBS spectra processing, and also detection and analysis of particles. Jean-Baptiste has been the coordinator of the French network on LIBS since 2013.

[a] Den – Service d'Etudes Analytiques et de Réactivité des Surfaces (SEARS), CEA, Université Paris-Saclay, F-91191 Gif sur Yvette, France.
[b] IVEA SAS, Centre Scientifique d'Orsay, Bât. 503, F-91400 Orsay, France.
[c] Univ.Grenoble Alpes, F-38000 Grenoble, France. CEA, LITEN, DTNM, NanoSafety Platform, F-38054 Grenoble, France.
[d] IRSN, PSN-RES, SCA, Aerosol Physics and Metrology Laboratory, F-91192 Gif-sur-Yvette, France.

1. Introduction

The intense development of industrial applications of engineered nanomaterials has led to their dissemination in our environment, which has been raising strong concerns about their potential adverse effects on human health. This issue is particularly acute for people who produce and handle those materials, who are obviously more exposed to inhalation, ingestion and penetration through the skin. To better evaluate and manage the risk induced by engineered nanomaterials, toxicological studies aim at characterizing their hazard, while in parallel different types of measurements are developed to assess the exposure, in particular at workplace. This latter topic was reviewed by Maynard et al. in 2007,[1] and more recently by Ding et al. in the context of industries and research laboratories.[2] Among the variety of nanomaterials produced, carbon nanotubes (CNTs) raise numerous questions due to their fibrous nature.[3] Different studies focused on exposure assessment to airborne CNTs.[4-8] As for other types of nanomaterials, one major challenge is to be able to measure the different properties of the nano-aerosol that may have an effect on the hazard: size, number and mass concentration, composition, shape, surface area, etc. As a matter of fact, the exposure assessment at workplace necessarily combines different techniques to quantify all measurands of interest.

Furthermore, the strategy also depends on the expected type of exposure, in relation with the ambient background level. For an acute exposure, for example due to an important leakage on a production process, a granulometer might be sufficient to trigger an alarm. But this is not an option for chronic exposure studies, for which the expected concentration in ambient air is much lower. In this case, filter sampling is necessary in order to accumulate enough material for analysis, and selectivity and sensitivity with respect to the ambient background are required. In addition to real-time measurements and samples observation by electron microscopic techniques, chemical analysis of the sampled material is an essential step to specifically identify, and further to quantify, the presence of airborne nanomaterials.[9] In particular, optical spectrometry, mainly Raman and fluorescence, X-ray fluorescence (XRF) spectrometries,[10-12] or ICP-MS[13] were used to analyze nanomaterials on a filter. However, as mentioned in ref. 5, those techniques raise the question of their routine onsite implementation for periodic exposure assessment.

Laser-induced breakdown spectroscopy (LIBS) is a well-known elemental analytical technique to do onsite or even in situ measurements. The analysis is fast, it is able to detect all elements, and the instrumentation can be compact. Those potential advantages make LIBS relevant for workplace monitoring. Therefore, in this paper we address the issue of exposure assessment to airborne CNTs by LIBS analysis of filter samples. Quantitative analysis of particles deposited on filters by LIBS was demonstrated by several teams, including in early publications by the group of Radziemsky on the detection of Be.[14] Neuhauser et al. obtained detection limits of heavy metals between several tens and several hundreds of ng/cm².[15] In their work, particles were collected on a filter band translated inside an exhaust duct of a waste incineration facility. 100 nm NaF particles were analysed on membrane filters with a limit of detection for F of 160 ng/cm² under helium atmosphere.[16] Metals in diesel particles collected in the exhaust gas of an engine were analyzed for different air/fuel ratios.[17] Size-resolved quantitative analysis of 14 elements deposited on successive collection plates of a cascade impactor was demonstrated by Kuhlen et al.[18] LIBS was also used to measure metals in PM_{10} sampled on a nylon membrane during Asian dust and pollution events.[19] Engineered TiO_2 and Fe_2O_3 nanomaterials sampled on filters were analyzed by Dewalle et al.[20] Nanoalloys and nanocomposites were recently characterized on silicon substrates.[21] In ref. 22, three portable techniques, LIBS, XRF and FTIR, were compared for assessment of exposure to TiO_2 nanoparticles sampled on polycarbonate filters. The LIBS detection limit was found to outperform that of XRF and FTIR by 2 to 3 orders of magnitude. To our knowledge, no study was published on CNTs sampled on filters. The only paper dealing with detection on CNTs by LIBS was proposed by R'mili et al., who demonstrated the real-time detection of micrometric CNTs bundles in direct analysis mode, i.e. by focusing the laser beam directly in the aerosol.[23]

Then, the objective of this work is to assess the performances of LIBS for onsite monitoring of chronic exposure to airborne CNTs. In particular, we aim at reaching a detection limit compliant with the exposure limit recommended by the NIOSH in 2013, of 1 µg/m³ for an 8-hour average during 45 years.[24] Yet, as carbon is a ubiquitous element in the environment, we focused on the analysis of metal impurities instead, Al and Fe in our case. To this end, we proceeded in three steps. First, we deposited lab-produced Al_2O_3 and Fe_2O_3 nanoparticles on 9 different types of filters to determine the most suitable one for low-level detection of both elements. Then, CNTs deposits were prepared on the selected filter, and their detection limit was determined in laboratory conditions. Eventually, we made an onsite measurement campaign in an industrial CNTs production plant to assess exposure in a real workplace. The final results of this study show that aerosolization of a few CNTs bundles inside the plant was detected, with an equivalent concentration 3 orders of magnitude lower than the exposure limit recommended by NIOSH.

2. Experimental

2.1 Samples

2.1.1 Deposition of oxide nanoparticles. In order to determine the detection limit of CNTs through the measurement of their Al and Fe impurities, a first series of experiments was conducted with Al_2O_3 and Fe_2O_3 nanoparticles deposited on different types of filters. The filters enrichment setup is shown in Fig. 1. A spark generator (GFG-1000, Palas) was used to

produce nanoparticles in argon, which were then transported in air with a 500 µg/m^3 and 700 µg/m^3 volume concentration (C_v) respectively for Al_2O_3 and Fe_2O_3 particles. A 4-way flow splitter enabled to deposit the particles on two filters in the same time. Both ways were equipped with a valve, a flow rate regulator and a pump. A third way was connected to a Tapered Element Oscillating Microbalance (TEOM 1105) measuring the deposited mass in real time. The flow rate in the three ways was Q = 3 L.min^{-1} and was regulated by a mass flow controller. The fourth way was used as an exhaust with a HEPA filter to prevent any release of nanoparticles in the ambient air. The deposited mass on the filter can be expressed as $m_{filter} = C_v.Q.\Delta t$ with Δt the enrichment time, and the mass density as $C_s = m_{filter}/S$ with S the filter exposed surface. The maximum enrichment time was 10 min, leading to a total deposited mass of Al or Fe on the filter of the order of 15-20 µg, as measured by the TEOM. This measurement was validated by duplicating several filters and ICP-OES analysis after filter dissolution. The deposit homogeneity was qualitatively controlled by SEM observations.

The filters had a 47 mm diameter and were of different nature: quartz fibres (Whatman QMA 1851 (QMA)), PTFE (Millipore FSLW (FS) and Pall Zefluor (Zefluor)), PVC (Pall GLA-5000 (PVC)), cellulose esters (Pall GN-4 Metricel (MEC), Millipore HAWP (HA) and Sartorius Sedim 11104 (CellAc)), and polycarbonate (Whatman Nuclepore (PC) and Millipore ATTP (ATTP)). In total, 9 different models of filters were tested. Except for the QMA filter, all of them were membrane filters with a thickness between 6 and 180 µm and a pore size between 0.2 and 5 µm. For the FS filter, only Al_2O_3 particles were deposited.

2.1.2 Deposition of CNTs. Commercial multiwall CNTs (Graphistrength C100, Arkema) with Al and Fe impurities were used in this study. Those impurities came from the Catalytic Chemical Vapor Deposition process used for CNTs production: Al was a growth medium residue, whereas Fe was a catalyst residue. Their concentration was stable in the powder, equal to 2.3% for Al and 1.9% for Fe (supplier data). After grinding and acid attack (H_2SO_4 / HNO_3) to increase their solubility, they were diluted and sonicated to be dispersed in water at a concentration of ca. 100 mg.L^{-1}, and then nebulized to deposit the CNTs on polycarbonate filters (Millipore GTTP, 37 mm diameter, 0.22 µm pore diameter, 25-30 µm thickness). By varying the exposure time between 1 and 60 minutes, the CNTs concentration on the filter could be estimated, and further validated by non-destructive total-reflection X-ray fluorescence (TXRF) measurements. The measured Fe concentration on the filter surface was between 0.4 and 6 ng/cm².

For carbon calibration, the same setup was used with QMA filters of 25 mm diameter. The enrichment time was between 1 and 30 minutes. Each filter was cut in two. One half was analysed by LIBS, the other half was measured by thermo-optical analysis. A Lab OC-EC Aerosol Analyzer (Sunset Laboratory Inc.) was used for that purpose, with the IMPROVE analysis protocol.[25] The deposited carbon mass was calibrated using a sucrose aqueous solution with a concentration of 10 g.L^{-1}. The total carbon concentration obtained on the filters was between 3 and 6 µg/cm².

2.1.3 Onsite measurements. The onsite campaign was realized in an industrial CNTs production plant. CNTs were synthesized inside a reactor by a Catalytic Chemical Vapor Deposition process. Then, CNTs were guided either to a barrelling workstation, where they were put into barrels for shipping, or to an extruder, where they were incorporated into a polymer matrix to form an extruded string that was subsequently granulated. CNTs were completely confined throughout the production and transport process within the plant, except for the barrelling and extrusion workstations. Therefore, we focused on those two places to measure a potential release of CNTs in the ambient air.

The barrelling workstation was surrounded by plastic blades, with an underpressure maintained inside by a ventilation system. A particle counter (Portable Aerosol Spectrometer, GRIMM) was used for continuous monitoring of the particles number density inside the workstation. During the barrelling operation, a barrel was connected to an isolation valve, filled with CNTs, then the valve was disconnected. This was done remotely from the outside of the workstation. In some cases, the operator had to wait until the particle number concentration had decreased below a predefined threshold value, and then he passed the arms through the plastic blades to put the barrel cover and get the barrel out of the workstation. This phase lasted approximately one minute and was the only moment when a potential release of CNTs inside the workstation might occur. Three sampling points were defined. The first one was the entrance of the extraction system inside the workstation (BW1). The second one was outside the workstation, at the height of respiratory airways of a man (BW2). The third one was the operator himself (BW3).

On the extrusion workstation, the CNTs feed system included a barrel of CNTs connected to a butterfly valve. The system was vibrated to inject CNTs at the extruder entrance, where they were mixed with a polymer matrix at an adjustable temperature. As this zone could potentially release CNTs in the ambient air, three extraction systems were placed above. At the other end of the extruder, the extruded string was granulated by a machine and the granules formed fell into barrels. At this point, CNTs were confined inside the polymer, but a very low risk of CNTs release could not be excluded. Three sampling locations were defined in the extrusion workstation: one above the incorporating zone (EW1), one close to the butterfly valve (EW2) and one close to the granulation machine (EW3). Finally, the centre of the plant was defined as the sampling point for background measurements (BG).

4 different sampling devices were used for the onsite measurement campaign:[26]

- A CATHIA sampler to measure the thoracic fraction of the aerosol.[27] The sampling flow rate was regulated by a critical orifice and a pump (Reciprotor).

- A button sampler with a portable pump (SKC) to measure the inhalable fraction of the aerosol.
- A "home-made" sampler with the shape of a Y, enabling to take two samples on 25-mm filter cassettes in the same time, with a single pump (Reciprotor).
- A portable aerosol sampler integrating a 1 $L.min^{-1}$ pump, a filter cassette with a 4-mm diameter inlet, and a cyclone with a 4 µm cutpoint (NANOBADGE - NanoInspect, Alcen Group, Paris and CEA, Grenoble).[28-29]

For all samplers, polycarbonate filters with 0.2 µm pore diameter were used (Millipore GTTP). Their diameter was 37 or 25 mm, depending on the system. The sampling points and sampling parameters are given in Table 1.

Table 1 Location and parameters of samples during the onsite measurement campaign.

Location		Sampling device	Flow rate ($L.min^{-1}$)	Duration (min)	Filter diameter (mm)	Reference
Barrelling	Inside (day 1)	Cathia	10.4	305	37	BW1a
	Inside (day 1)	Nanobadge	1	305	25	BW1b
	Inside (day 3)	Cathia	10.4	143	37	BW1c
	Outside (day 1)	Button	2	305	25	BW2a
	Outside (day 3)	Button	2	236	25	BW2b
	Operator (day 1)	Nanobadge	1	305	25	BW3
Extruder	Source (day 2)	Cathia	10	260	37	EW1a
	Source (day 2)	Nanobadge	1	260	25	EW1b
	Valve (day 2)	Button	2	260	25	EW2
	Granulation (day 2)	Cathia	10.4	260	37	EW3a
	Granulation (day 2)	Nanobadge	1	260	25	EW3b
Background	(day 2)	Home made	3	400	25	BGa
	(day 3)	Cathia	10	440	37	BGb

2.2 LIBS analysis

The LIBS system is presented in Fig. 2. It included a Nd:YAG laser at 355 nm (Brio, Quantel) with a 20 Hz repetition rate, a pulse duration of 5 ns FWHM and a maximum pulse energy of 25 mJ. An optical system was designed at the laser output to get a top-hat beam at the sample surface. Hence, the sample was ablated by a homogeneous circular laser spot of 220 µm diameter. An achromatic telescope was used to collect plasma emission and to inject it into an optical fibre with 0.22 numerical aperture, 910 µm core diameter and 1 m length. The fibre was connected to a 300 mm focal length spectrometer (SP2300i, Acton) with a slit width of 100 µm and a 2400 grooves/mm grating centred at 396.5 nm in order to simultaneously measure the sensitive Al lines at 394.40 and 396.15 nm, along with the Fe line at 404.58 nm. The resolving power of the system was $\lambda/\Delta\lambda$ = 5000 and the spectral bandwidth was 18 nm. The detector was an intensified CCD camera (iStar, Andor) with 2048x512 pixels of 13 µm. For calibration of C concentration on QMA filters, the spectrometer was centred at 183 nm in order to measure the C line at 193.09 nm.

For laboratory studies on oxide nanoparticles, measurements were performed with a pulse energy of 21 mJ (i.e. an irradiance of 11 GW/cm² on the sample), a gate delay of 1 µs after the laser pulse and a gate width of 1.5 µs. Those temporal parameters were optimized in order to maximize the signal-to-noise ratio of the Fe line. On each filter, a 25x25 matrix of single-shot spectra was recorded, with a 1 mm step between successive laser shots. The single-shot mode was compulsory for all membrane filters, since each individual laser shot drilled the filter. For QMA filters of 450 µm thickness, 3 laser shots could be accumulated at each point. The acquired spectra were subsequently summed line by line to get 25 replicates of 25 accumulated analysis points. For polycarbonate filters used for CNTs measurements, 20x20 single shot spectra were acquired, and summed 20 by 20. For QMA filters used for calibration of carbon, 6 replicates of 17 accumulated laser shots were recorded per filter.

For the onsite measurement campaign, a pulse energy of 17 mJ was used, with the same temporal parameters. Depending on the available filter surface, between 72 and 484 single-shot spectra were recorded. A measurement was defined as the accumulation of 22 laser shots. Therefore, the number of replicates was between 3 and 22 depending on the sample.

3. Results and discussion

3.1 Laboratory measurements of Al and Fe

The calibration curves of Al and Fe in deposits of oxide nanoparticles made in the laboratory were established for all types of filters, in order to determine the best one for CNTs low-level detection. Fig. 3 shows four of them, for HA, PC, PVC and QMA filters. Similar results, not shown, were obtained for the other filters. For each replicate, the line intensity was measured as the sum of 5 pixels centred on the line wavelength, then it was corrected for the background. For better readability, error bars represent ±2 standard deviations of the line net intensity, calculated from the 25 replicates. The low concentration range of calibration curves is fit by a line whose slope a is used to determine the limit of detection LOD according to the standard expression

$$LOD = 3\sigma_{blank}/a$$

where σ_{blank} is the standard deviation of the blank net intensity at the line wavelength. Two blank filters were measured: an unexposed filter and a filter exposed to dry air during 5 minutes (median enrichment time). The standard deviation was determined in both cases, respectively σ_0 and σ_5. σ_{blank} was calculated as the average of σ_0 and σ_5.

As shown in Fig. 3, all calibration curves are nonlinear. This is due to self-absorption of the sensitive chosen emission lines, and it is all the more pronounced for Al, since the 396.15 nm line is a resonant one. For the Fe 404.58 nm line, the lower level has an energy of 11976 cm^{-1}, relatively far from the fundamental level, therefore it is prone to self-absorption only for the most concentrated samples. For Al, we see that the calibration obtained on QMA filters is very bad, whereas the Fe calibration is correct. This is due to the fact that those quartz fibre filters are not free from aluminum, with an unknown and fluctuating concentration from one sample to the other. Therefore, there is an interference with the substrate that cannot be corrected. In addition, error bars are significantly larger for this type of filter than for the other ones. As error bars for Fe are comparable to other calibration curves, the ablation repeatability in the case of Al is not in question. This discrepancy is attributed to noise introduced by the background correction. As an example, for the filter with 690 ng/cm² of Al, the relative standard deviation (RSD) of the Al line net intensity was twice that of the raw intensity. In contrast, the RSD of the Fe line of the sample at 790 ng/cm² of Fe was almost the same before and after background correction. Finally, this clearly excludes QMA filters for analysis of Al-based nanoparticles.

Except for that particular case, the signal repeatability is satisfactory, with a typical RSD between 2% and 7% for all types of filters. Also, a good linearity is observed in the low concentration range.

Fig. 4 shows the detection limits obtained for all types of filters. We see that they lie between 0.8 and 2.4 ng/cm² for Al, and between 3.5 and 21 ng/cm² for Fe in our experimental conditions. As the background fluctuation was found similar for all membrane filters, the difference in the detection limit is attributed to the calibration line slope obtained in the low concentration range. Indeed, variations of the filter composition and microstructure leads to a different absorption efficiency of the laser energy and to a different interaction regime, therefore to a variable sensitivity from one filter to the other. To our knowledge, analysis of Al and Fe on filters was not published previously, but in comparison, the detection limits of other metals available in the literature extend from 10 to a few hundreds of ng/cm².[30-31] From the obtained surface detection limit LOD_s, the equivalent average concentration in the sampled air volume LOD_v can be calculated as $LOD_v = LOD_s.\pi/4.\phi^2/Q.\Delta t$, with ϕ the filter exposed diameter, Q the sampling flow rate and Δt the sampling duration. For a typical personal aerosol sampler such as the Nanobadge (see Table 1), with ϕ = 23 mm, Q = 1 $L.min^{-1}$ and Δt = 8h, a surface limit of detection of 1 ng/cm² is equivalent in the ambient atmosphere to about 8 ng/m^3.

In our case, the PC filter was found to be the one with the lowest detection limits both for Al and Fe. As our objective is to detect CNTs at a low concentration based on the analysis of their impurities at the percent level, the detection limit of those elements is the main choice criterion. In addition, in parallel with this study, non-destructive TXRF analyses were performed on several samples prior to LIBS measurements. PC filters are favourable for those analyses,[11] as they are very flat and smooth, and also easily observable by SEM. Therefore, in the following section, the analysis of Al and Fe in CNTs deposits was performed with PC filters.

3.2 Laboratory measurements of CNTs

3.2.1 Analysis of impurities. The concentration of Al and Fe impurities in CNTs deposited on polycarbonate filters was measured by LIBS. The calibration is shown in Fig. 5. The error bars represent ±1 standard deviation calculated from the 20 replicates. Note that the Al signal is plotted versus the Fe concentration, because on the one hand, only Fe could be measured by TXRF before LIBS analysis, and on the other hand, only the Al LIBS signal was detected. This is not surprising in view of the Fe concentration, close to the detection limit of this element determined previously, and taking into account that 20 laser shots per spectra, instead of 25, were accumulated.

Although the signal intensity on Fig. 5 seems to non-linearly depend on the concentration, no evidence of self-absorption was found. Indeed, the intensity ratio of both Al lines at 396.15 and 394.40 nm was found to be 2.17, 1.91 and 2.04 for the samples at 2.1, 4.2 and 6.2 ng/cm² respectively. Those values were not significantly different, and in very good agreement with the value expected when no self-absorption is present.[32] For lines of identical upper energy level, this theoretical ratio is the ratio of the lines strengths, in our case $(gA)_{396.15}/(gA)_{394.40}$ = 1.97, with A the Einstein coefficient and g the degeneracy level. Therefore, this nonlinearity was considered fortuitous and attributed to experimental error. Also, the non-zero intercept of the calibration line was attributed to a spectral interference of the Al 396.15 nm line with a molecular emission band, most probably from CN[33] and/or N_2[34]. Using the Al and Fe w/w fractions given in section 2.1.2, the detection limit was estimated at 1.1 ng/cm² of Al, which was consistent with the previous measurements, leading to an equivalent Al concentration in the atmosphere of 9.8 ng/m^3 in the same sampling conditions (23 mm, 1 $L.min^{-1}$, 8h), and an equivalent CNTs concentration of 0.43 µg/m^3. This result is compliant with the exposure limit recommended by the NIOSH for CNTs in workplace atmosphere cited in the introduction. In comparison, the detection limit of elemental carbon on a 25-mm filter by the reference method NIOSH 5040 is 90 ng/cm².[24] Therefore, LIBS is a suitable technique to monitor the presence of impurities in airborne particulate matter, such as CNTs, for occupational safety purposes.

3.2.2 Analysis of C. Being able to measure carbon itself would be relevant to monitor more pure CNTs, or other carbon-based

compounds (e.g. soot particles), or if the ambient atmosphere is filtered enough to reduce the ambient carbon background. In this case, polymer membrane filters are of course excluded, but QMA ones can be used, like for atmospheric aerosols measurements for instance.[35] Therefore, the CNTs deposits on QMA filters described in the experimental section were analysed by LIBS. Before that, the enrichment process had to be validated by a reference method. Fig. 6 shows the results of OC-EC analysis of the filters. It demonstrates that the elemental carbon concentration, i.e. the carbon nanotubes concentration, is well correlated to the enrichment time, and that the contribution of organic carbon is approximately constant, around 3 µg/cm², and predominant in the total carbon concentration. This organic carbon is the result of atmospheric CO_2 adsorption on quartz fibres. Its concentration in QMA filters depends on their storage conditions and duration. We note that a similar concentration was measured for an unexposed filter, meaning that the CNTs deposition protocol did not enrich the filter in additional organic carbon.

For LIBS measurements, the C 193.09 nm line was chosen instead of the more widespread 247.86 nm one. The excitation level is the same in both cases, but the 193.09 nm line has a 10 times higher transition probability. Although this gain was somewhat reduced due to the poor transmission efficiency of optical elements below 200 nm, the length of the optical fibre we used was relatively short (1 m), and the VUV line was found more sensitive than the UV one. Fig. 7 shows the carbon LIBS signal plotted against the total, organic and elemental carbon concentration. We see that the LIBS signal is not correlated to the total carbon, but to the elemental carbon, i.e. to the CNTs concentration on the filters. The following explanation is proposed: the vaporization efficiency of carbon from CNTs and of carbon from adsorbed CO_2 on quartz fibres is different. Therefore, the LIBS signal of carbon can be expressed as $I(C) = k_{CNT}.[C]_{CNT}.V_{ablated} + k_{CO2}.[C]_{CO2}.V_{ablated}$, with $k_{CNT} \neq k_{CO2}$. We checked that the silicon signal was constant for all samples, meaning that the ablated volume $V_{ablated}$ was constant from one filter to the other. And from Fig. 6, we see that the concentration of organic carbon is also approximately constant. Finally, the second term of the above equation is roughly constant, and we get a linear correlation of the LIBS signal with the CNTs concentration. This also justifies why the intercept of the linear fit is not zero: this is the organic carbon contribution.

The limit of detection of carbon on QMA filters is evaluated at 300 ng/cm² in our experimental conditions, leading to an equivalent concentration in the ambient atmosphere of 2.6 µg/m^3 with the same sampling parameters as previously. It is higher than the NIOSH recommended exposure limit (REL) for CNTs, but the measurement could be improved by accumulating more laser shots. However, we should emphasize that the quantitative analysis of elemental carbon, as demonstrated here, is only possible if the organic carbon contribution is constant for all samples or negligible. This was the case for CO_2 adsorbed in lab-prepared filters, whose contribution could be potentially measured on an unexposed part of the filter in addition to the analysis of the particles deposit. But this is not representative of atmospheric samples, for which a significant, and possibly highly fluctuating contribution of organic aerosols, would prevent any linear calibration. To overcome this limitation, filters could be heated in an oven at a suitable temperature under a controlled atmosphere to eliminate organic carbon prior to LIBS analysis, without modifying the elemental carbon.

3.3 Onsite measurement campaign

Having established that airborne CNTs sampled in representative conditions of a chronic exposure could be measured by LIBS with a sufficiently low detection limit, we implemented onsite sampling and analysis in an industrial CNTs production plant, as described in the experimental section. Yet, onsite samples revealed several issues. The first one was that the sampled material did not sufficiently adhere to the filter surface to undergo hundreds of laser shots. Indeed, the LIBS signal was found to decrease up to a factor of 3 during the acquisition, due to aerosolization of deposited particles by successive laser shots. Visual examination of the most enriched filters before and after analysis confirmed this hypothesis. Such a drift had not been observed with lab-prepared filters. Consequently, in order not to underestimate the measured concentration, only the first replicate, i.e. the first 22 laser shots, was used for quantitative measurements, assuming that it was the most representative of the initial state of the filter before analysis. Then, the error bar shown in the following was calculated as the standard deviation of the net signal over the 22 first single shots, divided by √22.

A second issue was that samples from the inside of the barrelling workstation were logically quite loaded with particles. As they were visibly black instead of white for lab-prepared, low concentrated samples, absorption efficiency of the laser radiation was much higher. So was the obtained signal, and we checked that the Al and Fe calibration previously obtained could not be used for those samples. Therefore, the LIBS measurement was re-calibrated using a single onsite representative sample that was analysed by ICP-OES, and assuming that the signal was linear over the calibration range. This assumption might be discussed in relation with the possibility of self-absorption with onsite samples. However, the re-calibration was performed with the second filter most concentrated in particles, yielding an Al concentration of 8.2 ng/cm². Over all onsite samples, this led to a maximum Al concentration measured of 13 ng/cm², approximately twice the maximum concentration of the calibration range shown on Fig. 5 for which no self-absorption was detected. In comparison, Fig. 3 shows that for oxide nanoparticles, self-absorption starts at a much higher concentration, of the order of 500 ng/cm² for PC filters. In addition, as shown in sections 3.1 and 3.2.1, a similar detection limit was obtained both for oxide nanoparticles and CNTs, meaning that the laser absorption efficiency is similar for both types of particles and that self-absorption might be expected for CNTs deposits at a comparable concentration level.

Therefore, we considered that the linearity assumption was reasonably valid for the onsite re-calibration.

Fig. 8 shows the measured concentrations of Al and Fe in onsite samples, in units of µg/m^3 in the ambient atmosphere, using sampling parameters of Table 1. The NIOSH REL for CNTs is also shown, considering a concentration of Al and Fe of 3.5% each in the CNTs produced in the plant, as measured by ICP-OES on production samples. The first three of them are samples from the inside of the barrelling workstation, where no operator is allowed to enter, the other ones are from other locations of the production plant, where the staff can move and carry out operations. A first comment can be made about the reproducibility of measurements, looking at two couples of samples taken in the same conditions after two days, BW1a/BW1c and BW2a/BW2b. Although error bars are large due to the low signal accumulation described above, measurements of day 1 and day 3 are within error bars, so the reproducibility was found satisfactory.

As expected, the first three samples exhibit the highest concentrations, with a value for Fe largely exceeding the REL for BW1a and BW1c. The difference between samples BW1a and BW1b, taken at the same place and at the same moment, is due to different sampling parameters and geometry. The CATHIA system has a horizontal slit that sampled the aerosol in the direction of the extraction flow, whereas the Nanobadge sampler was perpendicular to the flow, and with a sampling flow rate ten times lower. Therefore, the CATHIA collected more efficiently large, heavy particles, in this case CNTs bundles that were aerosolized during the barrelling operation, and found a higher concentration than the Nanobadge. In contrast to BW1 filters, all other samples in Fig. 8 show concentrations significantly below the REL, lower than 12 and 18 ng/m^3 respectively for Al and Fe, meaning that the exposure limit was fortunately not reached during normal operation in the CNTs production plant. Yet, a significant Al and Fe signal was detected, and taking into account the CNTs confinement throughout the plant and the sampling conditions inside the barrelling workstation and for other sampling locations, this signal was somewhat surprisingly high. Indeed, if there were CNTs on those filters, we could have expected that their concentration was several orders of magnitude lower than that of the first three ones, placed at the entrance of the extraction system inside the barrelling workstation. In addition, the Fe/Al ratio for those samples seems to vary much more than that of the BW1 filters. Therefore, our assumption was that the Al and Fe signal measured in the plant did not stem from CNTs, but mostly from other compounds present in the background atmosphere. This is likely, because both elements are frequently present in air at the µg/m^3 level, particularly in urban areas,[36-38] and then are not specific to CNTs.

The Fe/Al ratio was investigated to check if it could give a more peculiar information on the presence of CNTs. From Fig. 8, we determined that for filters exposed to CNTs it is between 3 and 4.5. The uncertainty on this ratio is quite high, but it is consistent with the 3.4 value measured by ICP-OES on a filter loaded with CNTs. Although both elements have an identical global concentration of 3.5% in CNTs, the Fe/Al ratio is significantly higher than 1 because Fe is a catalyst residue, present inside individual nanotubes, whereas Al is a residue of micrometric Al_2O_3 particles used as a growth medium for CNTs. Due to the mass of those particles, aerosolized CNTs are depleted in Al, and the sampled material is enriched in Fe. For other samples, the Fe/Al ratio spans from 0.7 to 2.5. Such a ratio is a coarse indicator, but it could help to selectively identify nanotubes with a better confidence than the mere Al or Fe concentration. However, one way to go further is to analyse the shot-to-shot correlation between the Al and Fe signals, shown in Fig. 9 for 3 samples: one from the ambient background in the production plant (BGa), one from the inside of the barrelling workstation (BW1a), for which the ambient background contribution is considered negligible, and one taken during granulation of the extruded string (EW3a). As one can see, no particular correlation is found for the ambient background, whereas a clear correlation can be observed from the BW1a sample. This correlation can be considered as the signature of CNTs, provided their concentration in Al and Fe does not change during production. Looking at the EW3a filter, we see that the obtained plot is a mixture of the two previous ones, with most laser shots showing no correlation like for the background filter, and a few ones exhibiting a correlation similar to that of the BW1a filter. This means that most of the Al and Fe signal for this sample came from the ambient background, and that a few CNTs bundles were sampled on this filter, yielding an abnormally intense LIBS signal with the characteristic Fe/Al correlation. This was supported by SEM observations of background samples and of the Nanobadge samples carried by the operator of the barrelling workstation, which found CNTs bundles with a size up to 20 µm. This confirmed that a very limited aerosolization of CNTs took place in the ambient atmosphere of the plant. However, the maximum CNTs concentration for those samples was estimated at 5 ng/m^3, well below the REL. Finally, the shot-to-shot analysis of the filters enabled to identify the presence of sparse CNTs bundles over the filter, which was not possible using the average Al and Fe concentration.

As a conclusion, this onsite measurements campaign was a success, as it showed that we were able to assess onsite the exposure to airborne CNTs in a production plant. Beyond that, the main feedback was that the choice of the filter, that had been defined from laboratory analyses, must be questioned, since it was found not suitable to correctly fix the sampled particles. In particular, the use of a fibre filter such as the QMA one can be raised again, since in this case particles are trapped in the filter volume rather than deposited on the surface, then aerosolization due successive laser shots might be less pronounced. Hence, aerosolization of CNTs powder could be done experimentally in order to better simulate the sampling, to better optimize the filter type, and to calibrate the measurement on more representative samples. For that purpose, different aerosolization devices were proposed in the literature for toxicological studies.[39-41]

4. Conclusions

The objective of this work was to assess the possibility of onsite monitoring of chronic exposure to airborne carbon nanotubes in a workplace atmosphere by LIBS analysis of filter samples. Due to the ubiquitous nature of carbon in the environment, CNTs metal impurities, Al and Fe, were chosen as elements of interest. We proceeded in three steps. We first evaluated the detection limit of both elements for different types of filters. LIBS analysis of lab-prepared Al_2O_3 and Fe_2O_3 nanoparticles deposits led to the selection of polycarbonate filters, that had a detection limit of 0.8 and 3.5 ng/cm² respectively for Al and Fe in our experimental conditions. This type of filter was then used to make controlled CNTs deposits, and we got an equivalent detection limit of 0.43 µg/m^3 of CNTs in ambient atmosphere, for sampling parameters typically used with personal samplers. This value is close to the NIOSH recommended exposure limit for CNTs, of 1 µg/m^3. Finally, a measurement campaign in an industrial CNTs production plant showed that onsite analysis was possible. All samples taken in the area accessible to workers exhibited an Al and Fe concentration much lower than the exposure limit. Yet, by analysing the shot-to-shot correlation of Al and Fe LIBS signals, we showed that most part of the measured Al and Fe concentration stemmed from the background, and we were able to identify a few CNTs bundles sampled on different filters. The equivalent CNTs concentration in the workplace atmosphere was nearly 3 orders of magnitude lower than the exposure limit.

Those results demonstrated that LIBS is a suitable technique to perform airborne nanoparticles monitoring with a detection limit compliant with current recommendations, even in the case when the target elements are ubiquitous, and with a possibility to extract maximum information from the samples when shot-to-shot spectra are analysed. Of course the task will be all the easier if discriminant elements are measured, like for example Co, used as a catalyst of CNTs growth in different processes[42] or in composite nanotubes,[43] whose concentration in the ambient atmosphere must be negligible, or B in boron nitride nanotubes,[44] or Ce in CeO_2 nanoparticles.[45] Compared to the TXRF technique, also implemented for laboratory or onsite direct analysis of filters, LIBS has a comparable detection limit,[10-11] with the additional possibility to measure light elements such as carbon, as exemplified in this paper.

Acknowledgements

This work was part of the GENESIS project (Global Evaluation of Nanocomposites for Emerging Safe Industrial Solutions) supported by OSEO (France).

References

1 A. D. Maynard and R. J. Aitken, *Nanotoxicology*, 2007, **1**, 26.
2 Y. Ding et al., *Journal of Hazardous Materials*, 2017, **322**, 17.
3 A. Genaidy, T. Tolaymat, R. Sequeira, M. Rinder and D. Dionysiou, *Science of the Total Environment*, 2009, **407**, 3686.
4 A. D. Maynard, P. A. Baron, M. Foley, A. A. Shvedova, E. R. Kisin and V. Castranova, *Journal of Toxicology and Environmental Health, Part A*, 2004, **67**, 87.
5 R. Tantra and P. Cumpson, *Nanotoxicology*, 2007, **1**, 251.
6 J. H. Lee et al., *Inhalation Toxicology*, 2010, **22**, 369.
7 K. Aschberger, H. J. Johnston, V. Stone, R. J. Aitken, S. M. Hankin, S. A. K. Peters, C. Lang Tran and F. M. Christensen, *Critical Reviews in Toxicology*, 2010, **40**, 759.
8 A. Meyer-Plath et al., *Annual World Conference on Carbon - Carbon 2015*, Dresden, Germany.
9 M. Ono-Ogasawara, F. Serita and M. Takaya, *J. Nanopart. Res.*, 2009, **11**, 1651.
10 L. Borgese, A. Zacco, S. Pal, E. Bontempi, R. Lucchini, N. Zimmerman and L. E. Depero, *Talanta*, 2011, **84**, 192.
11 S. Motellier, K. Lhaute, A. Guiot, L. Golanski, C. Geoffroy and F. Tardif, *J. Phys.: Conf. Ser.*, 2011, **304**, 012009.
12 Y. Kayser, J. Sá and J. Szlachetko, *Nanoscale*, 2015, **7**, 9320.
13 Y.-K. Hsieh, L.-K. Chen, H.-F. Hsieh, C.-H. Huang and C.-F. Wang, *J. Anal. At. Spectrom.*, 2011, **26**, 1502.
14 D. A. Cremers and L. J. Radziemski, *Appl. Spectrosc.*, 1985, **39**, 57.
15 R. E. Neuhauser, U. Panne and R. Niessner, *Anal. Chim. Acta*, 1999, **392**, 47.
16 M. Tran, B. W. Smith, D. W. Hahn and J. D. Winefordner, *Appl. Spectrosc.*, 2001, **11**, 1455.
17 K. Lombaert, S. Morel, L. Le Moyne, P. Adam, J. Tardieu de Maleissye and J. Amouroux, *Plasma Chemistry and Plasma Processing*, 2004, **24**, 41.
18 T. Kuhlen, C. Fricke-Begemann, N. Strauss and R. Noll, *Spectrochimica Acta Part B*, 2008, **63**, 1171.
19 J.-H. Kwak, G. Kim, Y.-J. Kim and K. Park, *Aerosol Science and Technology*, 2012, **46**, 1079.
20 P. Dewalle, J.-B. Sirven, A. Roynette, F. Gensdarmes, L. Golanski and S. Motellier, *J. Phys.: Conf. Ser.*, 2011, **304**, 012012.
21 S. A. Davari, S. Hu and D. Mukherjee, *Talanta*, 2017, **64**, 330.
22 R. F. LeBouf, A. L. Miller, C. Stipe, J. Brown, N. Murphy and A. B. Stefaniak, *Environ. Sci.: Processes Impacts*, 2013, **15**, 1191.
23 B. R'mili, C. Dutouquet, J.-B. Sirven, O. Aguerre-Chariol and E. Frejafon, *J. Nanopart. Res.*, 2011, **13**, 563.
24 NIOSH current intelligence bulletin, 2013, **65**.
25 J. C. Chow, J. G. Watson, D. Crow, D. H. Lowenthal and T. Merrifield, *Aerosol Science and Technology*, 2001, **34**, 23.
26 J. C. Volkwein, A. D. Maynard and M. Harper, in *Aerosol Measurement: Principles, Techniques, and Applications,* 2011, John Wiley & Sons.
27 J. F. Fabriès, P. Görner, E. Kauffer, R. Wrobel and J C. Vigneron, *Ann. Occup. Hyg.*, 1998, **42**, 453.
28 C. Asbach et al., *Science of the Total Environment*, 2017, **603–604**, 793.
29 B. Faure, H. Dozol, C. Brouard, A. Guiot and S. Clavaguera, *J. Phys.: Conf. Ser.*, 2017, **838**, 012006.
30 U. Panne, R. E. Neuhauser, M. Theisen, H. Fink and R. Niessner, *Spectrochimica Acta Part B*, 2001, **56**, 839.
31 R. Chinni, D. A. Cremers and R. Multari, *Appl. Opt.*, 2010, **49**, C143.
32 N. Konjevic, M. Ivkovic and S. Jovicevic, *Spectrochimica Acta Part B*, 2010, **65**, 593.
33 S. Trautner, J. Jasik, C. G. Parigger, J. D. Pedarnig, W. Spendelhofer, J. Lackner, P. Veis, J. Heitz, *Spectrochimica Acta Part A*, 2017, **174**, 331.
34 H. Nassar, S. Pellerin, K. Musiol, O. Martinie, N. Pellerin and J.-M. Cormier, *J. Phys. D: Appl. Phys.*, 2004, **37**, 1904.
35 J. J. Cao, S. C. Lee, K. F. Ho, X. Y. Zhang, S. C. Zou, K. Fung, J. C. Chow and J. G. Watson, *Atmospheric Environment*, 2003, **37**, 1451.
36 N. A. H. Janssen et al., *Atmospheric Environment*, 1997, **31**, 1185.

37 D. Voutsa, C. Samara, Th. Kouimtzis and K. Ochsenkühn, *Atmospheric Environment*, 2002, **36**, 4453.
38 M. Nishikawa, I. Matsui, D. Batdorj, D. Jugder, I. Mori, A. Shimizu, N. Sugimoto and K. Takahashi, *Atmospheric Environment*, 2011, **45**, 5710.
39 P. A. Baron, G. J. Deye, B. T. Chen, D. E. Schwegler-Berry, A. A. Shvedova and V. Castranova, *Inhalation Toxicology*, 2008, **20**, 751.
40 T. Myojo, T. Oyabu, K. Nishi, C. Kadoya, I. Tanaka, M. Ono-Ogasawara, H. Sakae and T. Shirai, *J. Nanopart. Res.*, 2009, **11**, 91.
41 O. L. C. Le Bihan, A. Ustache, D. Bernard, O. Aguerre-Chariol and M. Morgeneyer, *Journal of Nanomaterials*, 2014, 193154.
42 M. Nath, B. C. Satishkumar, A. Govindaraj, C. P. Vinod and C. N. R. Rao, *Chem. Phys. Lett.*, 2000, **322**, 333.
43 S. Liu, J. Zhu, Y. Mastai, I. Felner and A. Gedanken, *Chem. Mater.*, 2000, **12**, 2205.
44 N. G. Chopra, R. J. Luyken, K. Cherrey, V. H. Crespi, M. L. Cohen, S. G. Louie and A. Zettl, *Science*, 1995, **269**, 966.
45 M. Leppänen, J. Lyyränen, M. Järvelä, A. Auvinen, J. Jokiniemi, J. Pimenoff and T. Tuomi, *Nanotoxicology*, 2012, **6**, 643.

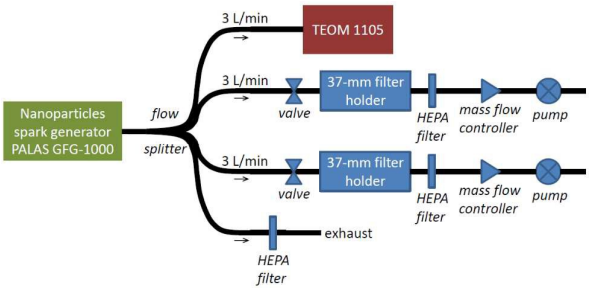

Figure 1 Experimental setup for depositing Al_2O_3 and Fe_2O_3 nanoparticles on filters

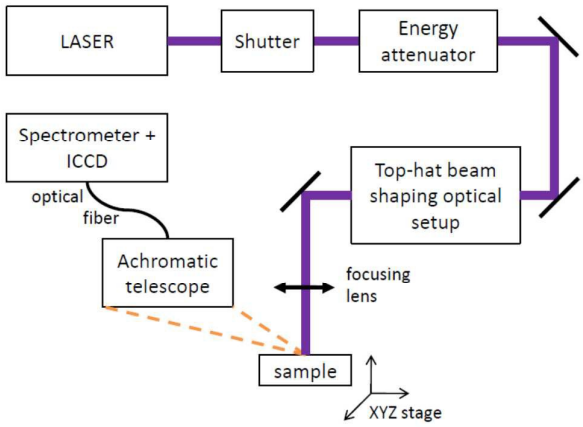

Figure 2 Experimental setup for LIBS measurements

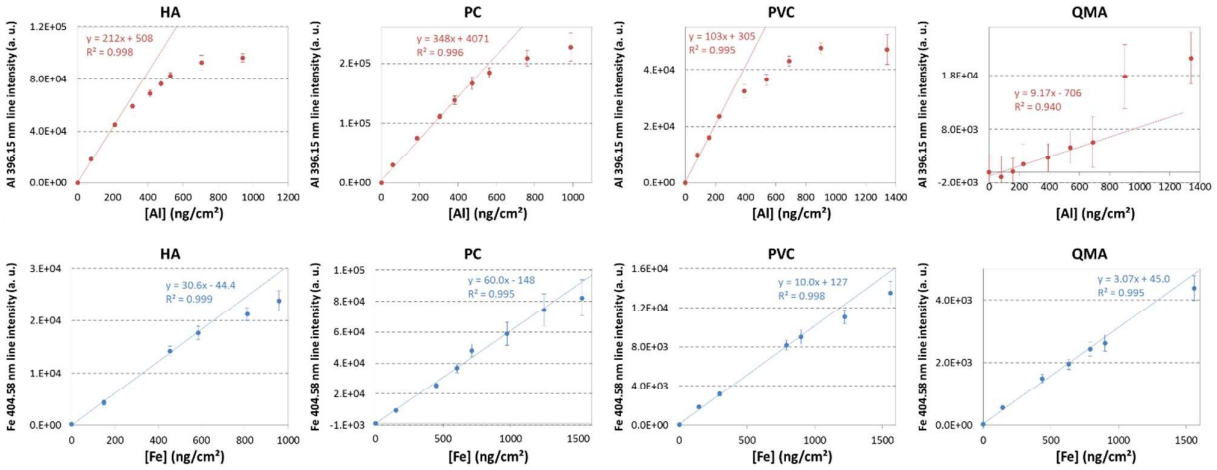

Figure 3 Calibration of Al (top) and Fe (bottom) concentration in deposits of oxide nanoparticles, for 4 types of filters (HA, PC, PVC, QMA)

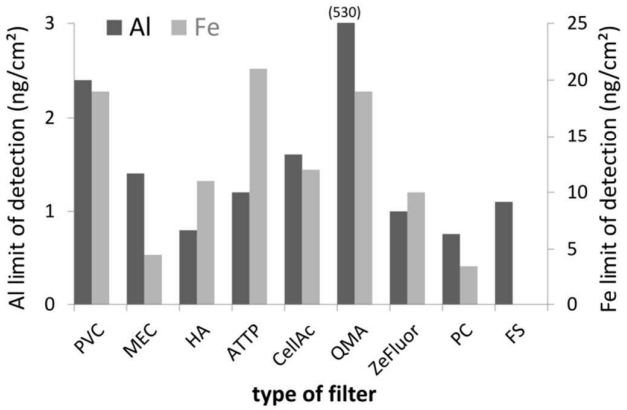

Figure 4 Limits of detection of Al and Fe in deposits of oxide nanoparticles on 9 types of filters

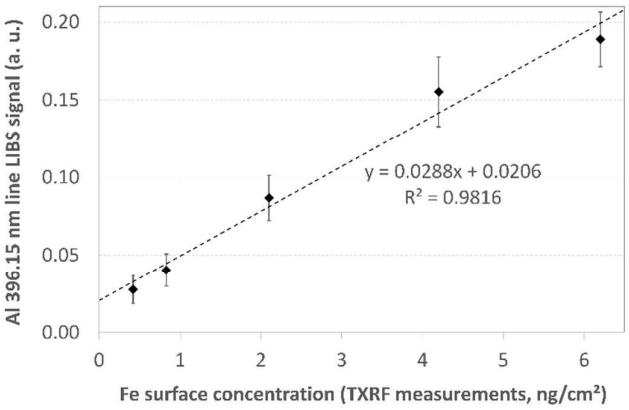

Figure 5 Calibration of Fe concentration in carbon nanotubes deposits on polycarbonate filters

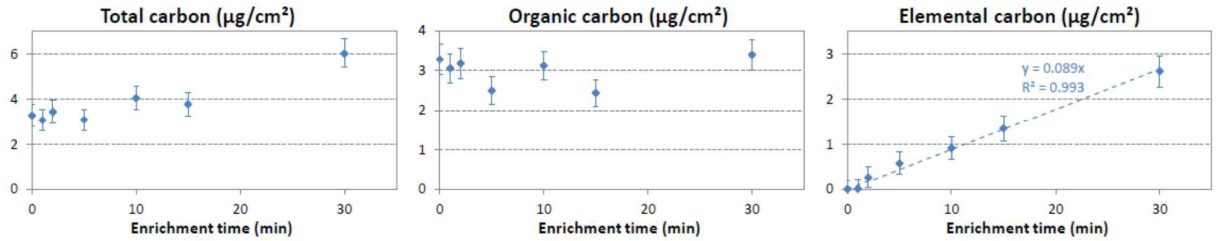

Figure 6 Total (left), organic (centre) and elemental (right) carbon concentration measured by thermo-optical analysis of quartz fibres filters enriched with carbon nanotubes, as a function of the enrichment time

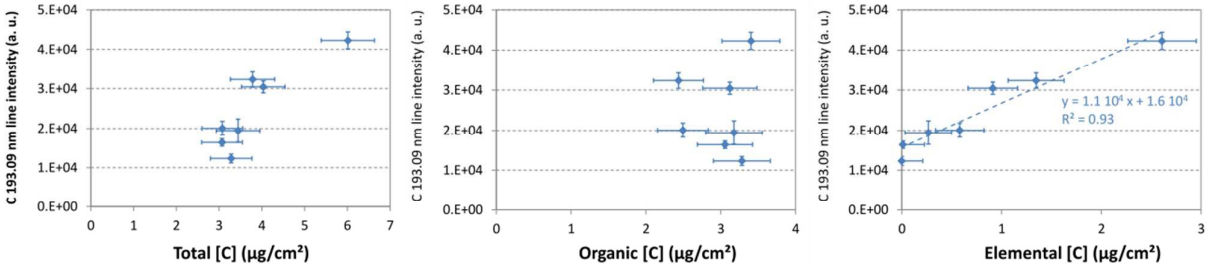

Figure 7 LIBS signal of carbon measured on quartz fibres filters, as a function of the total (left), organic (centre) and elemental (right) carbon concentration

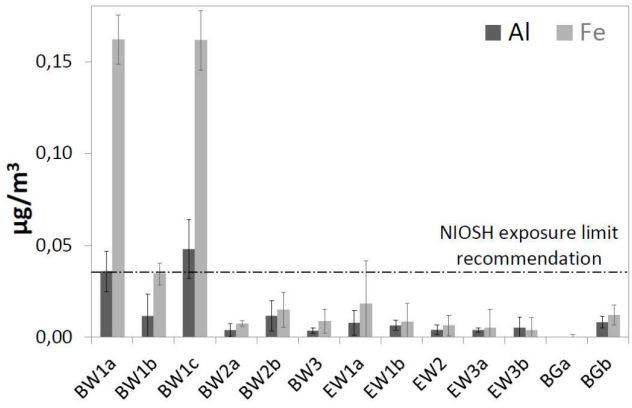

Figure 8 Concentration of Al and Fe measured by LIBS in the atmosphere of different sampling locations of an industrial CNTs production plant (see Table 1)

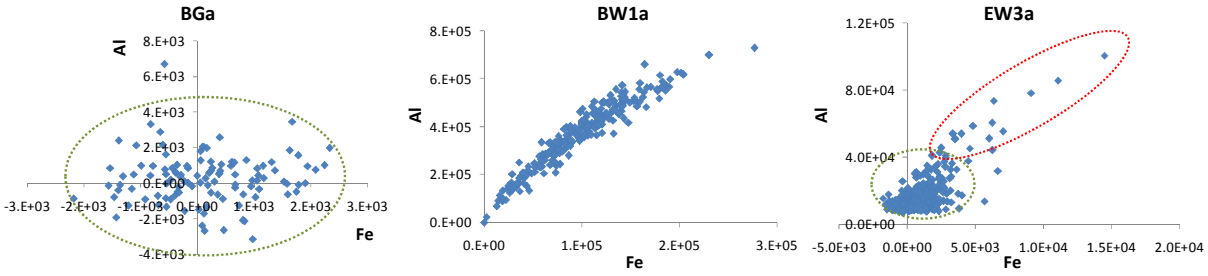

Figure 9 Shot-to-shot Al signal intensity versus Fe signal intensity, for three samples: BGa (background), BW1a (inside of the barrelling workstation), and EW3a (granulation process)

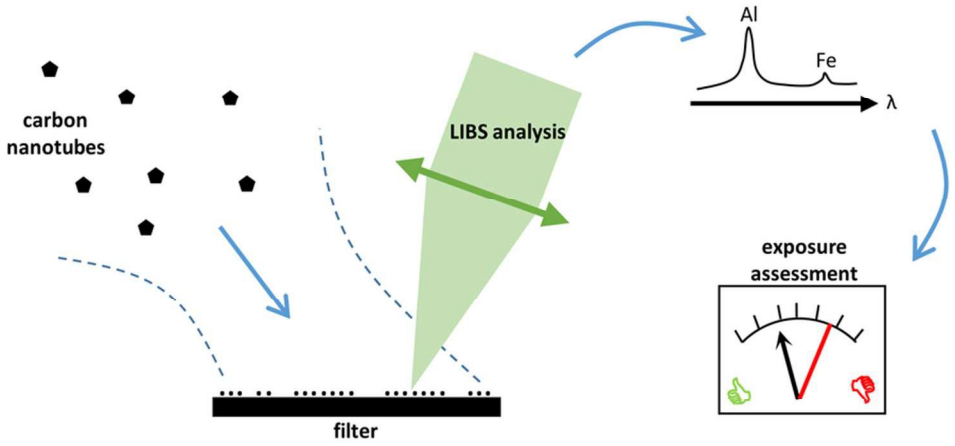

Airborne carbon nanotubes sampled on filter are quantified in a workplace atmosphere by LIBS analysis of their metal impurities

40x20mm (600 x 600 DPI)